12th IFAC International Symposium on
Advanced Control of Chemical Processes
July 14-17, 2024. Toronto, Canada

Dynamic mode decomposition based MPC of fluidized bed spray agglomeration

E. Otto * **R. Dürr** ** **A. Bück** *** **A. Kienle** *,****

* *Otto von Guericke University Magdeburg,39106 Magdeburg, Germany (e-mail: eric.otto@ovgu.de)*
** *Magdeburg-Stendal University of Applied Sciences, 39114 Magdeburg, Germany (e-mail: robert.duerr@h2.de)*
*** *Friedrich-Alexander-University Erlangen-Nuremberg, 91058 Erlangen, Germany (e-mail: andreas.bueck@fau.de)*
**** *Max-Planck-Institute for Dynamics of Complex Technical Systems, 39106 Magdeburg, Germany (e-mail: kienle@mpi-magdeburg.mpg.de)*

Abstract: Fluidized bed spray agglomeration (FBSA) is an efficient particle formation process for the production of granules extensively used in the food, agricultural and pharmaceutical industry. Specifications on agglomerate properties such as the agglomerate size determine the quality of the product and can be controlled by varying different process conditions. In this contribution data-driven model predictive control (MPC) of the average agglomerate size is presented. Dynamic mode decomposition (DMD) is used to identify a linear model of the process dynamics from snapshot measurements of the particle size distribution. Using DMD as system identification technique eliminates the complex process of identifying a mechanistic process model and at the same time includes advantageous model order reduction for the MPC application. The DMD model is obtained from simulated data and validated against a second, independent, data set. Subsequently, the model is deployed in an MPC controller, which is tested in a simulation study, showing promising performance in set point tracking and disturbance rejection scenarios.

Keywords: Control of particulate processes, Data-driven control, Model-predictive control, Linear system identification, Model order reduction

1. INTRODUCTION

Solid raw materials for industrial and other applications often come in granular form. Since certain granule properties such as volume, shape and porosity determine the economic value of the product, particle formation processes that produce granules with predefined properties are required. In fluidized bed spray agglomeration (FBSA), agglomerates are formed from primary particles with the help of a liquid binding agent containing a solid material either solved or dispersed. To this end, a particle bed is fluidized and the binding agent is sprayed on the particle surface. Initially, after collision, liquid bridges connect the primary particles. Evaporation of the liquid to the fluidization air results in the formation of solid bridges and the final agglomerate (Fig. 1). In the continuous process configuration, as presented in Fig. 2, primary and product particles are continuously fed and withdrawn, respectively, resulting in higher production rates compared to the batch process.

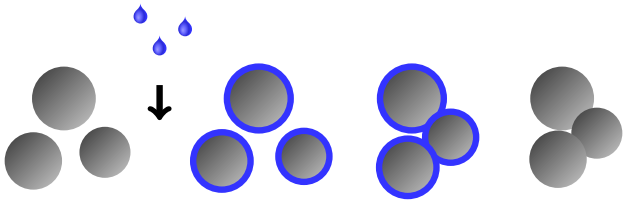

Fig. 1. Agglomeration process with surface wetting due to binder addition, collision of wet particles and formation of a new agglomerate due to binder drying.

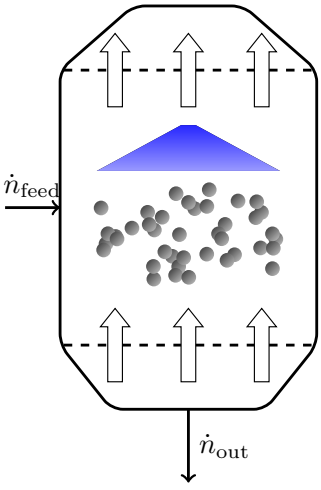

Fig. 2. Process scheme with particle feed, agglomeration in the process chamber and particle withdrawal.

Agglomerate properties depend on various parameters and conditions of the formation process. Specifically for continuous FBSA, experimental investigations highlighted the influence of process conditions such as fluidization gas temperature, binder spray rate and binder solids concentration on the particle size distribution and other properties (Strenzke et al., 2020).

In combination with model-based process control strategies, these dependencies can be leveraged for the production of high-value, tailor-made agglomerates. Since the particle size, represented by agglomerate volume, is the most important product property, this contribution will focus on it. Control of particle size during the size-enlargement process has been investigated for agglomeration in pans or drums (Pottmann et al., 2000; Glaser et al., 2009; Vesjolaja et al., 2020) and fluidized beds (Cotabarren et al., 2015; Bück et al., 2016; Otto et al., 2022). Several of these contributions apply linear model predictive control (MPC) which is an established, optimization-based control technique and has many advantages over classical control strategies such as PID-control. This includes the possibility of controlling complex, multi-variable systems, explicitly considering constraints on inputs and states and incorporating economic considerations. However, compared to PID control it requires a process model with predictive accuracy at least over a certain time horizon. Due to the computational complexity of underlying optimization in MPC application, low-dimensional models are crucial. For FBSA processes, however, the distributed and therefore infinite-dimensional nature of the particle property distributions generally results in high-dimensional model approximations. Furthermore, precise control-oriented models are difficult to obtain from mechanistic modeling due to the complexity of the involved subprocesses. Therefore, data driven methods for process modeling represent a promising alternative over first-principle modeling (Pitchaiah and Armaou, 2010; Arbabi et al., 2018; Son et al., 2022).

Dynamic mode decomposition (DMD) (Tu et al., 2014) is a technique that combines data driven modeling with dimensionality reduction, yielding a linear time-invariant (LTI) process model from data snapshots. In addition to the dimensionality reduction, DMD has two main advantages for the application in linear MPC. The overall effort of obtaining a model that is readily applicable in an MPC controller is small compared to modeling strategies requiring mechanistic considerations. Furthermore, the connection of the DMD algorithm to Koopman operator theory offers a simple way to extend the method presented here, and find improved process models by means of nonlinear measurements (Williams et al., 2015).

In this work, a DMD model for a continuous FBSA process is computed and validated, based on data from dynamic simulations with measurement noise. Using the DMD model, an MPC controller is designed for the process. The MPC controller is validated in dynamic simulation with respect to its set point tracking and disturbance rejection performance.

2. PROCESS MODEL

In this contribution, agglomerates are characterized by their volume v. This allows convenient modeling of the process via population balance modeling, resulting in a population balance equation (PBE) with v as internal coordinate. In the following the equations are described briefly. The model is an adapted version of the ones presented in Otto et al. (2021, 2022). For more details the reader is referred to these publications.

The dynamics of the number density distribution (NDD) $n(t,v)$ of agglomerates in the agglomeration chamber

$$\frac{\partial n(t,v)}{\partial t} = \dot{n}_\mathrm{f}(t,v) + \dot{n}_\mathrm{a}(t,v) - \dot{n}_\mathrm{o}(t,v) \tag{1}$$

are obtained by balancing the the particle feed $\dot{n}_\mathrm{f}(t,v)$, binary aggregation $\dot{n}_\mathrm{a}(t,v)$ and the particle withdrawal $\dot{n}_\mathrm{o}(t,v)$. The agglomeration term

$$\begin{aligned}\dot{n}_\mathrm{agg}(t,v) = \; & \frac{1}{2}\int_0^v \beta(t,u,v-u)n(t,u)n(t,v-u)\,\mathrm{d}u \\ & - \int_0^\infty \beta(t,v,u)n(t,v)n(t,u)\,\mathrm{d}u\,,\end{aligned} \tag{2}$$

describes the size-enlargement due to 'birth' and 'death' of agglomerates after aggregation. The kinetics of these processes are described by the agglomeration kernel $\beta(t,u,v)$, generally depending on various process conditions and material parameters. In Otto et al. (2021) the three empirical parameters a, b and β_0 of the so-called Kapur kernel

$$\beta(t,u,v) = \beta_0 \frac{(uv)^a}{(u+v)^b}. \tag{3}$$

have been correlated with different process parameters based on continuous FBSA experiments (Strenzke et al., 2020). Selecting the gas inlet temperature T_g as manipulated variable, agglomeration kinetics can be parametrized as follows:

$$\beta_0 = 10^{k_1 T_\mathrm{g} + k_2} \tag{4}$$

$$a = 0 \tag{5}$$

$$b = k_3 T_\mathrm{g} + k_4. \tag{6}$$

The primary particle feed distribution $\dot{n}_\mathrm{f}(v)$ is assumed to be normally distributed around an average particle volume v_feed with constant particle flow rate

$$\dot{n}_\mathrm{f}(v) = N_\mathrm{f} \exp\left(\frac{(v-v_\mathrm{feed})^2}{\sigma_\mathrm{feed}^2}\right). \tag{7}$$

In the Strenzke et al. (2020) experiments, the particle outlet

$$\dot{n}_\mathrm{o}(t,v) = KT(v)n(t,v) \tag{8}$$

is realized by a countercurrent air flow, resulting in internal classification with separation function $T(v)$ and outlet rate K which is assumed to be constant. Both, $T(v)$ and K have been determined empirically in Otto et al. (2021) from particle size measurements of the particle outlet.

Since the NDD is generally not completely controllable, it is reasonable to control an average value. Therefore, we choose the so called Sauter mean diameter d_{32} as measured output variable to control. It is an industrially relevant particle size measure, which is proportional to the ratio of total particle volume to surface, i.e.

$$d_{32} = 6\frac{V_\mathrm{tot}}{A_\mathrm{tot}}. \tag{9}$$

Under the assumption of spherical particles, d_{32} is computed directly from the NDD $n(v)$.

For the dynamic simulation and subsequent system identification and control, Eq. (1) is discretized at $N = 300$ points using a finite volume scheme (Singh et al., 2016), resulting in a system of ODEs solved in MATLAB.

3. METHODS

3.1 Dynamic mode decomposition

Dynamic mode decomposition (DMD) is a data-driven system identification and model order reduction method aiming at finding a linear model from snapshot data (Tu et al., 2014). Originally developed for autonomous systems, its extension, dynamic mode decomposition with control (DMDc) can also be applied to systems with input signals (Proctor et al., 2016). DMDc aims at finding reduced order approximations of the matrices $\mathbf{A}$ and $\mathbf{B}$ that fit the linear model

$$x_{k+1} = \mathbf{A}x_k + \mathbf{B}u_k \tag{10}$$

to a sequence of state and input snapshots

$$\mathbf{X} = [x_1 \ x_2 \ \dots \ x_{N_t}] \in \mathbb{R}^{N_x \times N_t} \tag{11}$$

$$\mathbf{X}' = [x_2 \ x_3 \ \dots \ x_{N_t+1}] \in \mathbb{R}^{N_x \times N_t} \tag{12}$$

$$\mathbf{\Upsilon} = [u_1 \ u_2 \ \dots \ u_{N_t}] \in \mathbb{R}^{N_u \times N_t}, \tag{13}$$

which can be reformulated as

$$\mathbf{X}' = \mathbf{A}\mathbf{X} + \mathbf{B}\mathbf{\Upsilon}. \tag{14}$$

The DMDc algorithm is build upon the truncated singular value decompositions of the augmented data matrix $\mathbf{\Omega}$ and of the data matrix of the output space $\mathbf{X}'$, given by

$$\mathbf{\Omega} := \begin{bmatrix} \mathbf{X} \\ \mathbf{\Upsilon} \end{bmatrix} \approx \tilde{\mathbf{U}}\tilde{\mathbf{\Sigma}}\tilde{\mathbf{V}}^* \tag{15}$$

$$\mathbf{X}' \approx \hat{\mathbf{U}}\hat{\mathbf{\Sigma}}\hat{\mathbf{V}}^*. \tag{16}$$

The right-hand-sides of (15) and (16) are the optimal rank p, respectively rank r, approximations of $\mathbf{\Omega}$ and $\mathbf{X}'$. Choosing p and r is crucial, in order to capture all the actual system dynamics without the effect of noise. Using Eqs. (15) and (16), the least-square optimal matrices $\mathbf{A}$ and $\mathbf{B}$ are approximated by the low-dimensional matrices

$$\mathbf{A} \approx \tilde{\mathbf{A}} = \hat{\mathbf{U}}^*\mathbf{X}'\hat{\mathbf{V}}\tilde{\mathbf{\Sigma}}^{-1}\tilde{\mathbf{U}}_1^*\hat{\mathbf{U}} \in \mathbb{R}^{r\times r}$$

$$\mathbf{B} \approx \tilde{\mathbf{B}} = \hat{\mathbf{U}}^*\mathbf{X}'\hat{\mathbf{V}}\tilde{\mathbf{\Sigma}}^{-1}\tilde{\mathbf{U}}_2^* \in \mathbb{R}^{r\times l}.$$

resulting in the low-dimensional dynamical system

$$\tilde{x}_{k+1} = \tilde{\mathbf{A}}\tilde{x}_k + \tilde{\mathbf{B}}u_k. \tag{17}$$

The transformation matrix from low to high-dimensional state space is given by $\hat{\mathbf{U}}$, i.e.

$$x_k = \hat{\mathbf{U}}\tilde{x}_k. \tag{18}$$

In order to identify the linear dynamics, it can be beneficial to enrich the measured data using delay coordinates (Tu et al., 2014), i.e. stacking N_d time-delayed versions of $\mathbf{X}$ in the augmented data matrix

$$\mathbf{X}_{\text{aug}} = \begin{bmatrix} x_1 & x_2 & \dots & x_{N_t-N_d} \\ x_2 & x_3 & \dots & x_{N_t-N_d+1} \\ \dots & \dots & \dots & \dots \\ x_{N_d+1} & x_{N_d+2} & \dots & x_{N_t} \end{bmatrix} \in \mathbb{R}^{N_d N_x \times N_t}. \tag{19}$$

Repeating this procedure for the input matrix, the DMD algorithm is then performed on $\mathbf{X}_{\text{aug}}$, $\mathbf{X'}_{\text{aug}}$ and $\mathbf{\Upsilon}_{\text{aug}}$.

Originally, DMD has been used as a computationally efficient method to analyze flow patterns in fluid dynamics, where the eigenvalues λ and eigenvectors φ of the system matrix $\mathbf{A}$ are of interest. The eigenvectors are termed dynamic modes and can be obtained with little computational effort from the singular values and vectors given above. In the present contribution, we are only interested in the matrix $\tilde{\mathbf{A}}$, therefore the computation of the dynamic modes is omitted.

Besides the general advantages of using data driven process models, the advantages of using a DMDc model for MPC in the agglomeration context are twofold. On the one hand, the linearity of the process model simplifies the application since it is advantageous for the solution of the underlying optimization problem. On the other hand, the low dimension of the reduced model enables real time computation of the control action.

In order to improve the quality of the DMD model and prepare it for application in the linear control context, some data preprocessing is required. Dynamic mode decomposition is known to provide biased results in the presence of sensor noise, in fact, the eigenvalues of the identified system matrix are shifted to be more stable (Dawson et al., 2016). Although different extensions of DMD are available to compensate for the effect of noise, none of these are readily applicable to the dynamic mode decomposition with control algorithm. Thus, in this contribution the data snapshots with added white Gaussian noise will be filtered before a DMD model is computed. Furthermore, the state and input snapshots are shifted around steady state values resembling the desired operating point. Finally, since control inputs and states differ in some order of magnitudes both values are scaled appropriately for improved numerical stability.

3.2 Linear model predictive control

Linear model predictive control aims at finding a sequence of controller outputs $\{u_k\}$ minimizing a cost function J, that depends on system state predictions over certain number of future time instants N_p (Kouvaritakis and Cannon, 2016). For set point tracking and disturbance rejection, deviations of the system output from the desired operating point y_d are minimized. The predictions of the states $\{x_k\}$ are computed using a linear process model. Finally, the minimization problem is subject to inequality constraints, i.e. the admissible interval of input values $[u_\text{min}, u_\text{max}]$, resulting in the following summarized formulation:

$$\begin{aligned} \min_{\{u_k\}} \quad & J = \sum_{k=0}^{N_\text{p}} e_k^\intercal Q e_k + u_k^\intercal R u_k \\ \text{s. t.} \quad & x_{k+1} = \tilde{\mathbf{A}}x_k + \tilde{\mathbf{B}}u_k, \\ & y_k = \tilde{\mathbf{C}}x_k, \\ & e_k = y_k - y_{\text{d},k}, \\ & u_\text{min} < u_k < u_\text{max}. \end{aligned} \tag{20}$$

Here Q and R are positive semi-definite weighting matrices, used to weight the control error and energy respectively. The time step is indexed by k and N_p is the number of prediction time steps computed. The optimization problem above is solved iteratively at every time instant and only the first value of the optimal input sequence $\{u_k\}$ is actually implemented at the plant. One of the advantages of MPC is the flexibility of formulating the cost function and therefore the possibility to incorporate various control goals. Additionally, constraints on states and inputs can easily be incorporated. Closed-loop stability of finite-

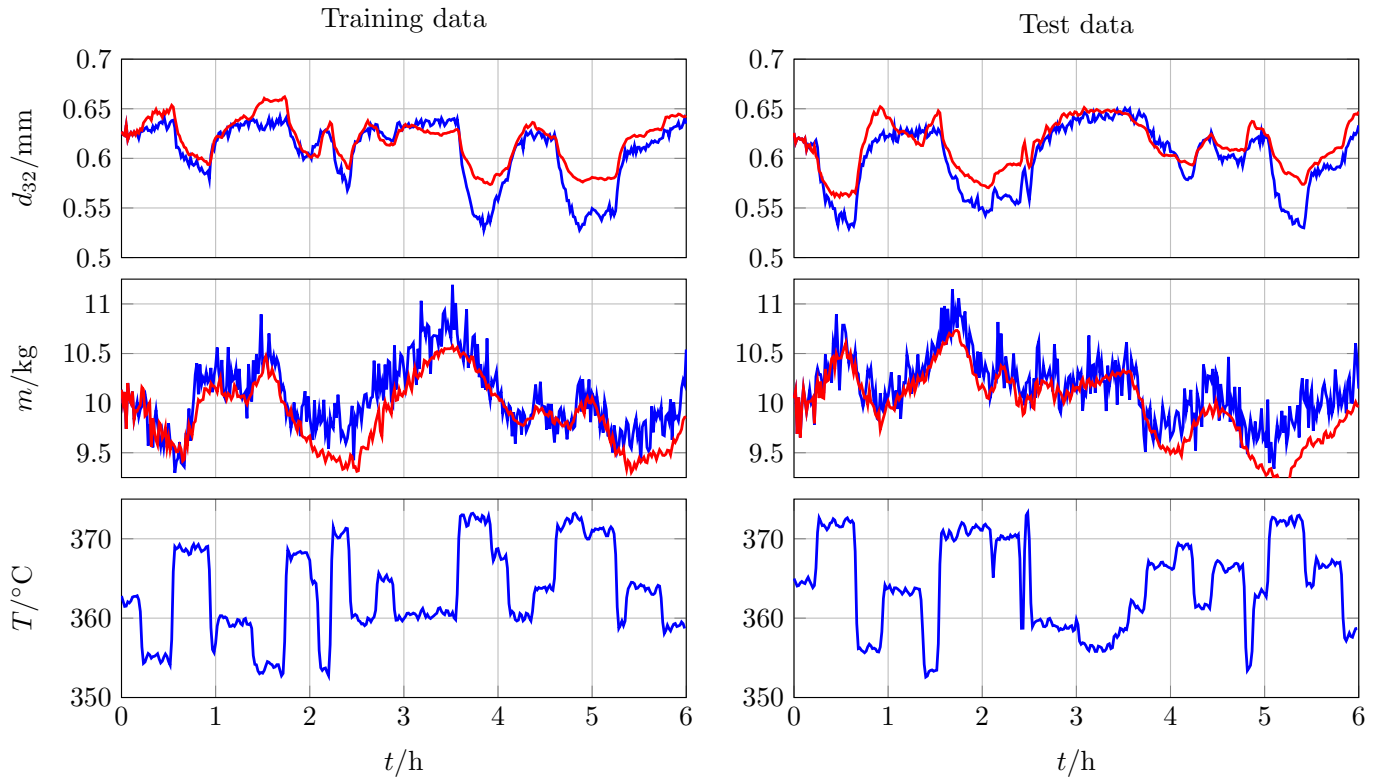

Fig. 3. Comparison between data (blue) and model predictions (red). **Left:** Training data and model predictions. **Right:** Validation data and model predictions. **From top to bottom:** Sauter mean diameter d_{32} and total bed mass m, Gas inlet temperature T_g.

horizon MPC without specific terminal cost, is generally not given, however by a sufficiently large choice of the prediction horizon N_p, stability can usually be met (Mayne et al., 2000).

4. RESULTS

4.1 Agglomeration modeling using DMD

In order to obtain a data set for the training of the DMD model, the population balance equation presented above is simulated over a time horizon of $T = 6$ h. For the sequence of inputs a piece wise constant signal is generated. The amplitudes are chosen randomly within the plant-specific restrictions. The time intervals between changes of amplitude are also chosen randomly. The choice of a suitable sampling interval t_s depends on various factors. It is limited by the specific particle size measurement device but has be small enough to capture the relevant dynamics of the process. Additionally, in an MPC application it is crucial for the real-time capability since it is the maximum time to solve the underlying optimization problem. With respect to these restrictions, a sampling time of $t_s = 60$s has been chosen. In order to simulate a more realistic scenario, white Gaussian noise is added to the input and state variables. It should be noted that it is generally also possible to generate the required data from experiments.

After applying the DMD algorithm to the data with $N_d = 4$ time delays, i.e. to a 1200-dimensional state, a 235-dimensional reduced order state transition matrix $\tilde{\mathbf{A}}$ is obtained. The value of N_d has been determined iteratively and provides the best compromise between model accuracy and dimension. In order to validate the DMD model, a second validation data set is generated. Both data sets are compared with the respective model predictions in Fig. 3. As comparison variables, the Sauter mean diameter, i.e. the control variable and the total mass of agglomerates in the bed m are chosen. With respect to prediction accuracy over the course of 6 hours, the model performs qualitatively well both on the training as well as on the validation set, indicating general validity for input sequences of this specific type. This is true for the Sauter mean diameter as well as the total bed mass. The 4 hour horizon over which the DMD model achieves low-error predictions suggest that the model is suitable for a MPC application. It should be noted, however, that the input sequences generated by the model predictive controller will generally differ from the type used here. Thus, it is crucial to do closed-loop validation of the model as aprt of the overall control system. The DMD model parameters are summarized in Tab. A.2 in the appendix.

4.2 Particle size control with linear MPC

The DMD model defined by the state transition matrix $\tilde{\mathbf{A}}$ and the input matrix $\tilde{\mathbf{B}}$ is utilized to control the Sauter mean diameter d_{32} by means of MPC. To this end, the model has to be augmented by an output matrix $\tilde{\mathbf{C}}$ which is obtained by linearizing the output equation (Eq. (9)). The MPC algorithm is implemented in MATLAB using its native model predictive control toolbox, where the constrained quadratic programming problem is solved by

an active set algorithm. The current state is measured, transformed to the low dimensional state $\tilde{x}$ by Eq. (18) and used as initial value for the prediction. Alternatively, if no measurement is available, it can be observed, e.g by the built-in Kalman filter. The admissible interval of the manipulated variable $T_g \in [353\,\mathrm{K}, 373\,\mathrm{K}]$ is determined by practical considerations regarding the safe and stable operation of the agglomeration plant (Strenzke et al., 2020). With a prediction horizon of $N_p = 30$ time steps, i.e. 30 min, a good dynamic response to reference and disturbance steps is obtained, also stability of the control system is promoted. On a AMD Ryzen 9 7950X 16 core processor, we observe a MPC step computation time less than 10 % of the sample time, hence the computational feasibility is ensured. The controller parameters are summarized in Tab. A.3 in the appendix.

The MPC controller is validated in dynamic simulations. Fig. 4 displays the closed-loop response to several reference steps. The controlled process follows an increase of the desired Sauter mean diameter from 0.6 mm to 0.65 mm. The rate of convergence is, however, limited by the fact that T_g is in saturation during the larger part of the time interval. A subsequent decrease of d_{32} to 0.55 mm, on the other hand, is achieved quickly. A possible approach to deal with the temperature restriction to improve closed-loop performance is to augment the system by additional manipulated variables such as the primary particle feed rate or the binder spray rate. This would also allow for a cost function formulation that incorporates energy efficiency considerations.

In order to investigate the closed-loop disturbance response, it is assumed that the average diameter of the primary particles d_{feed} is varied. In Fig. 5 variations from 0.2 mm to 0.3 mm and 0.15 mm are presented. The controller is able to suppress the disturbances quickly with moderate control action.

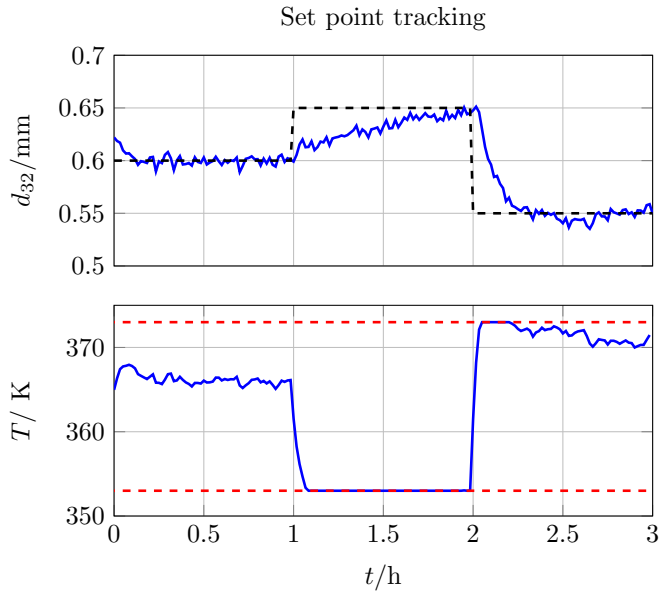

Fig. 4. Set point tracking of the MPC controller. **Top:** Controlled Sauter mean diameter (blue) with desired set point (black). **Bottom:** Manipulated variable T_g (blue) with upper and lower bounds (red).

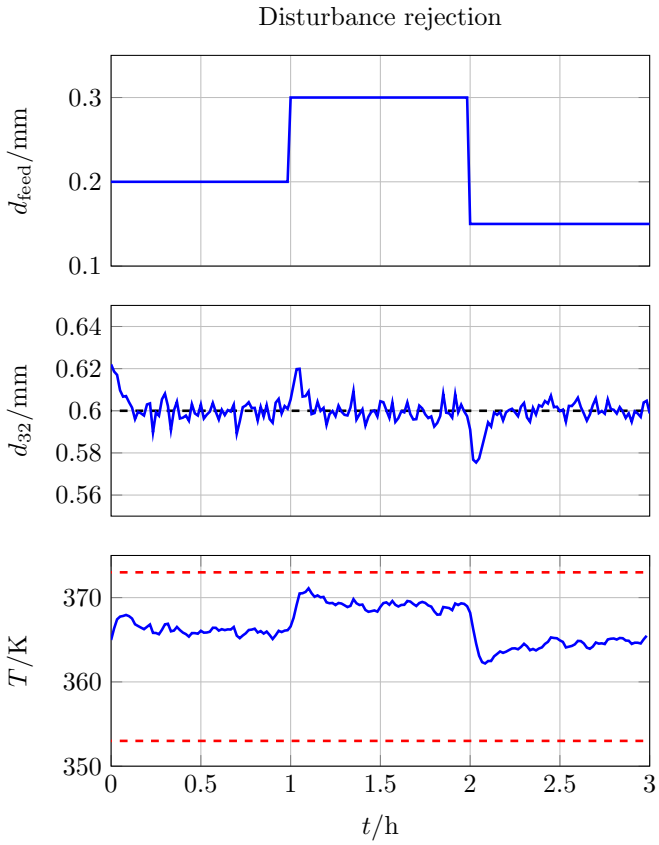

Fig. 5. Disturbance rejection of the MPC controller. **Top:** Disturbed variable. **Middle:** Controlled Sauter mean diameter (blue) with desired set point (red). **Bottom:** Manipulated variable T_g (blue) with upper and lower bounds (red).

5. CONCLUSION AND OUTLOOK

In this contribution model predictive control for the average agglomerate size in a fluidized bed spray agglomeration process has been presented. The underlying process model has been identified from data snapshots using dynamic mode decomposition. The linear DMD model achieves a good prediction of the average agglomerate size while having a low dimension and is therefore suitable for MPC. Tested by means of dynamic simulations, the DMD based controller achieves good results in reference tracking and disturbance rejection scenarios.

Future research directions are manifold. It will be advantageous to pursue additional control goals such as keeping the bed mass within certain boundaries for stable plant operation, controlling the width of the particle size distribution for improved product quality as well as optimizing the process from an economic perspective. To this end, additional input variables such as the primary particle feed and the binder spray rate have to be considered, i.e. the DMD model has to be adapted and reevaluated. Additional practically relevant extensions of the process model are the incorporation of the porosity as internal agglomerate property and augmenting the plant by a particle recycle for improved efficiency. Finally, in order to improve the model prediction quality, the DMD algorithm can be extended methodologically to approximate Koopman

eigenfunctions (Williams et al., 2015) and thereby achieve a better linear approximation of the highly nonlinear dynamics. Finally, experimental validation of the proposed control scheme is planned.

ACKNOWLEDGEMENTS

This work is funded by the DFG SPP 2364 "Autonomous processes in particle technology" (project ID: 504524147). The financial support is hereby gratefully acknowledged.

REFERENCES

Arbabi, H., Korda, M., and Mezić, I. (2018). A data-driven koopman model predictive control framework for nonlinear partial differential equations. In *2018 IEEE Conference on Decision and Control (CDC)*, 6409–6414. doi:10.1109/CDC.2018.8619720.

Bück, A., Dürr, R., Schmidt, M., and Tsotsas, E. (2016). Model predictive control of continuous layering granulation in fluidised beds with internal product classification. *Journal of Process Control*, 45, 65–75. doi: https://doi.org/10.1016/j.jprocont.2016.07.003.

Cotabarren, I.M., Bertín, D.E., Bucalá, V., and Piña, J. (2015). Feedback control strategies for a continuous industrial fluidized-bed granulation process. *Powder Technology*, 283, 415–432. doi: https://doi.org/10.1016/j.powtec.2015.06.010.

Dawson, S.T.M., Hemati, M.S., Williams, M.O., and Rowley, C.W. (2016). Characterizing and correcting for the effect of sensor noise in the dynamic mode decomposition. *Experiments in Fluids*, 57(42). doi: https://doi.org/10.1007/s00348-016-2127-7.

Glaser, T., Sanders, C.F., Wang, F., Cameron, I.T., Litster, J.D., Poon, J.M.H., Ramachandran, R., Immanuel, C.D., and Doyle, F.J. (2009). Model predictive control of continuous drum granulation. *Journal of Process Control*, 19(4), 615–622. doi: https://doi.org/10.1016/j.jprocont.2008.09.001.

Kouvaritakis, B. and Cannon, M. (2016). *Model Predictive Control: Classical, Robust and Stochastic*. Springer International Publishing. doi: https://doi.org/10.1007/978-3-319-24853-0 ,.

Mayne, D., Rawlings, J., Rao, C., and Scokaert, P. (2000). Constrained model predictive control: Stability and optimality. *Automatica*, 36(6), 789–814. doi: https://doi.org/10.1016/S0005-1098(99)00214-9.

Otto, E., Behrens, J., Palis, S., Dürr, R., and Kienle, A. (2022). Discrepancy-based control of particle processes. *Journal of Process Control*, 110, 99–109. doi: https://doi.org/10.1016/j.jprocont.2021.11.014.

Otto, E., Dürr, R., Strenzke, G., Palis, S., Bück, A., Tsotsas, E., and Kienle, A. (2021). Kernel identification in continuous fluidized bed spray agglomeration from steady state data. *Advanced Powder Technology*, 32(7), 2517–2529. doi: https://doi.org/10.1016/j.apt.2021.05.028.

Pitchaiah, S. and Armaou, A. (2010). Output feedback control of distributed parameter systems using adaptive proper orthogonal decomposition. *Industrial & Engineering Chemistry Research*, 49(21), 10496–10509. doi: 10.1021/ie100463f.

Pottmann, M., Ogunnaike, B.A., Adetayo, A.A., and Ennis, B.J. (2000). Model-based control of a granulation system. *Powder Technology*, 108(2), 192–201. doi: https://doi.org/10.1016/S0032-5910(99)00220-X.

Proctor, J.L., Brunton, S.L., and Kutz, J.N. (2016). Dynamic mode decomposition with control. *SIAM Journal on Applied Dynamical Systems*, 15(1), 142–161. doi: 10.1137/15M1013857.

Singh, M., Kumar, J., Bück, A., and Tsotsas, E. (2016). A volume-consistent discrete formulation of aggregation population balance equations. *Mathematical Methods in the Applied Sciences*, 39(9), 2275–2286. doi: https://doi.org/10.1002/mma.3638.

Son, S.H., Choi, H.K., Moon, J., and Kwon, J.S.I. (2022). Hybrid koopman model predictive control of nonlinear systems using multiple edmd models: An application to a batch pulp digester with feed fluctuation. *Control Engineering Practice*, 118, 104956. doi: https://doi.org/10.1016/j.conengprac.2021.104956.

Strenzke, G., Dürr, R., Bück, A., and Tsotsas, E. (2020). Influence of operating parameters on process behavior and product quality in continuous spray fluidized bed agglomeration. *Powder Technology*, 375, 210–220. doi: https://doi.org/10.1016/j.powtec.2020.07.083.

Tu, J.H., Rowley, C.W., Luchtenburg, D.M., Brunton, S.L., and Kutz, J.N. (2014). On dynamic mode decomposition: Theory and applications. *Journal of Computational Dynamics*, 1(2), 391–421. doi: 10.3934/jcd.2014.1.391.

Vesjolaja, L., Glemmestad, B., and Lie, B. (2020). Double-loop control structure for rotary drum granulation loop. *Processes*, 8(11). doi:10.3390/pr8111423.

Williams, M.O., Kevrekidis, I.G., and Rowley, C.W. (2015). A data–driven approximation of the koopman operator: Extending dynamic mode decomposition. *Journal of Nonlinear Science*, 25, 1307–1346. doi: https://doi.org/10.1007/s00332-015-9258-5.

Appendix A. PARAMETERS

Table A.1. PBE parameters.

Parameter	Symbol	Value
Prim. part. volume	v_{feed}	0.0042 mm^3
Withdrawal rate	K	0.0008 s^{-1}
Kernel parameter	k	[-72.27, 0.157, 3.24, -0.00827]

Table A.2. DMD model parameters.

Parameter	Symbol	Value
Sample time	t_{s}	60 s
Number of discretized states	N_x	300
Number of snapshots	N_t	360
Number of time delays	N_d	4
Number of inputs	N_u	1
DMD truncation value	p	236
DMD truncation value	r	235

Table A.3. MPC parameters.

Parameter	Symbol	Value
Sample time	t_{s}	60 s
Manipulated variable minimum	$u_{\min}$	353 K
Manipulated variable maximum	$u_{\min}$	373 K
Prediction horizon	N_{p}	30
Control horizon	N_{c}	15
Control variable weight	Q	1
Manipulated variable weight	R	0.1